Macedonian Journal of Chemistry and Chemical Engineering, Vol. **44**, No. 2, pp. xx–xx (2025)

MJCCA9 –

ISSN 1857-5552
e-ISSN 1857-5625

Received: March 5, 2025
Accepted: April 15, 2026

DOI: 10.20450/mjcce.2026.3471
Original scientific paper

QUALITY BY DESIGN APPROACH TO THE DEVELOPMENT OF METFORMIN HYDROCHLORIDE GRANULES WITH IMMEDIATE AND PROLONGED RELEASE

Maja Todeska[1], Daniel Velickovski[1], Martina Gjorgjevska[1], Dragana Petrushevska[1], Teodora Tasevska[1], Lina Livrinska Trpeska[1], Nikola Geskovski[1*], Katerina Goracinova[1], Emilija Atanasovska[2], Maja Simonoska Crcarevska[1*]

[1]Faculty of Pharmacy, Ss. Cyril & Methodius University in Skopje, Majka Tereza 47, 1000 Skopje, Republic of North Macedonia
[2]Faculty of Medicine, Ss. Cyril & Methodius University in Skopje, 50 Divizija 6, 1000 Skopje, Republic of North Macedonia

ngeskovski@ff.ukim.edu.mk; msimonoska@ff.ukim.edu.mk

Metformin hydrochloride (MHCl) is administered at high doses and requires robust formulation strategies to balance rapid drug availability with controlled-release performance. This study applied a Quality by Design (QbD) framework to develop immediate-release (IR) and prolonged-release (PR) MHCl granules and to evaluate the impact of binder selection on product quality and release behavior. Formulations were produced via wet granulation using polyvinylpyrrolidone (PVP), gelatin, and pregelatinized starch 1500 as binders. PR granules were further coated with Eudragit® RS/RL using a fluid-bed process. Risk assessment tools (Ishikawa and FMECA) guided the identification of critical quality attributes (CQAs), critical material attributes (CMAs), and critical process parameters (CPPs). Compatibility studies confirmed the absence of drug–excipient interactions. All IR formulations demonstrated rapid dissolution (> 90 % release within 5 min). Uncoated PR granules exhibited partial release control, while coated formulations showed binder-dependent differences in particle size distribution and dissolution performance. The gelatin-based PR formulation provided the most consistent release profile and the closest alignment with United States Pharmacopeia (USP) extended-release criteria, as it demonstrated low variability and minimal intermediate-point deviations. The study confirmed that binder selection was a high-impact critical material attribute for achieving robust prolonged-release MHCl granules within a QbD-driven development strategy.

Keywords: metformin hydrochloride; Quality by Design; wet granulation; binder selection; prolonged-release granules; fluid-bed coating

КВАЛИТЕТ ПРЕКУ ДИЗАЈН ПРИСТАП ЗА РАЗВОЈ НА ГРАНУЛИ СО МЕТФОРМИН ХИДРОХЛОРИД СО БРЗО И ПРОДОЛЖЕНО ОСЛОБОДУВАЊЕ

Метформин хидрохлорид (MHCl) се администрира во високи дози и бара робустни формулациски стратегии за да се постигне рамнотежа помеѓу брзата достапност на лекот и контролираното ослободување. Во оваа студија беше применет пристапот „Квалитет преку дизајн“ (QbD) за развој на гранули на MHCl со брзо ослободување (IR) и продолжено ослободување (PR), како и за проценка на влијанието на изборот на врзувач врз квалитетот на производот и профилот на ослободување. Формулациите беа подготвени со влажна гранулација користејќи поливинилпиролидон (PVP), желатин и прежелатинизиран скроб 1500 како врзувачи. PR гранулите дополнително беа обложени со Eudragit® RS/RL со примена на флуид-бед техника. Алатките за проценка на ризик (Ишикава дијаграм и FMECA) беа искористени за идентификација на критичните атрибути на квалитет (CQA), критичните атрибути на материјалите (CMA) и критичните процесни параметри (CPP). Студиите за компатибилност потврдија дека нема

интеракции помеѓу лекот и помошните супстанции. Сите IR формулации покажаа брзо ослободување (> 90 % во рок од 5 минути). Необложените PR гранули покажаа делумна контрола на ослободувањето, додека обложените формулации покажаа разлики во однос на распределбата на големината на честичките и брзината на ослободување во зависност од типот на врзувачот. Формулацијата базирана на желатин обезбеди најконзистентен профил на ослободување и најдобро усогласување со критериумите за продолжено ослободување наведени во американската фармакопеја (United States Pharmacopeia), со ниска варијабилност и минимални отстапувања во меѓуточките. Студијата потврди дека изборот на врзувач е критичен атрибут на материјал со значително влијание за постигнување робустни гранули на MHCl со продолжено ослободување во рамки на QbD пристапот.

Клучни зборови: метформин хидрохлорид; квалитет преку дизајн; влажна гранулација; избор на врзувач; гранули со продолжено ослободување; обложување со флуид-бед

1. INTRODUCTION

Type 2 diabetes mellitus (T2DM) is a progressive metabolic disorder characterized by insulin resistance and impaired glucose metabolism. It accounts for approximately 95 % of all diabetes cases and affects over 800 million people worldwide as of 2024. Among the available therapies, metformin hydrochloride (MHCl), a hydrophilic biguanide derivative, remains the first-line pharmacological treatment.[1,2]

MHCl primarily suppresses hepatic gluconeogenesis, enhances peripheral insulin sensitivity, and reduces intestinal glucose absorption. Long-term clinical studies have confirmed its ability to lower glycosylated hemoglobin (HbA1c), reduce cardiovascular morbidity, and improve body weight and lipid profiles, with a minimal risk of hypoglycemia.[3]

Despite these advantages, MHCl requires relatively high daily doses (500–2250 mg), which creates formulation and patient compliance challenges. Large tablet sizes and high drug-to-excipient ratios can complicate administration, particularly in geriatric patients and individuals with dysphagia.[4] Recognizing these issues, the U.S. Food and Drug Administration (FDA) issued guidance in 2015 emphasizing the importance of solid oral dosage form characteristics, such as size, shape, and swallowability, as determinants of adherence. Consequently, alternative delivery approaches are needed to overcome the limitations of conventional MHCl tablets while maintaining efficacy and safety.[5,6]

Oral granules represent a versatile and patient-friendly alternative to conventional solid dosage forms. They enable flexible dose titration, can be administered after reconstitution in water or by being mixed with soft food, and allow for the modulation of drug release profiles, making them particularly suitable for pediatric and geriatric populations.[7]

MHCl is classified as a Biopharmaceutics Classification System (BCS) Class III drug, indicating high aqueous solubility but low intestinal permeability. Its absorption is, therefore, permeability-limited rather than dissolution-limited, suggesting that formulation strategies should ensure rapid dissolution while potentially prolonging mucosal contact to optimize bioavailability.[8] However, MHCl granulation is challenging due to its high water solubility (> 300 mg/ml), hygroscopicity, poor compressibility, and tendency to agglomerate.[6] To achieve immediate-release (IR) or prolonged-release (PR) profiles, the careful selection of binder type and concentration is essential, as these factors influence granule integrity, drug release kinetics, and process performance.

The Quality by Design (QbD) framework, as outlined in International Council for Harmonisation of Technical Requirements for Pharmaceuticals for Human Use (ICH) Q8(R2),[9] offers a structured, science-based approach to pharmaceutical development. QbD involves defining a Quality Target Product Profile (QTPP), identifying Critical Quality Attributes (CQAs), and applying risk assessment tools, such as Ishikawa diagrams and Failure Modes, Effects, and Criticality Analysis (FMECA), to determine Critical Material Attributes (CMAs) and Critical Process Parameters (CPPs). This systematic strategy supports the establishment of a design space, robust process control, and regulatory compliance.

The objective of this paper was to implement a QbD framework[9,10] in the formulation of MHCl granules for immediate-release and prolonged-release oral administration. Three pharmaceutical binders, polyvinylpyrrolidone (PVP), gelatin, and pregelatinized starch 1500, were selected based on their physicochemical and regulatory suitability for wet granulation. Granules were prepared by manual wet granulation and characterized for key CQAs, including particle size (PS), particle

size distribution (PSD), bulk and tapped density, moisture content, drug content uniformity, and dissolution performance. A structured risk assessment was performed to evaluate the impact of binder type and process parameters on product quality and to establish control strategies supporting robust formulation design. This work provides a risk-informed, binder-focused application of QbD implementation in early-stage pharmaceutical development, aiming to enhance process understanding and rational formulation design for patient-compliant MHCl granule dosage forms.

2. EXPERIMENTAL SECTION

2.1. *Materials*

Metformin hydrochloride (MHCl) (kindly donated by Alkaloid AD, Skopje, North Macedonia) was used as the active pharmaceutical ingredient. Excipients included α-lactose monohydrate (VWR, Germany) and microcrystalline cellulose (MCC) (FMC, USA) as fillers; croscarmellose sodium (Barentz, Netherlands) and sodium starch glycolate (Merck, Germany) as superdisintegrants; sucrose (Merck, Germany) as a sweetener; and talc (Interhem, North Macedonia) as glidant and lubricant. Binders were polyvinylpyrrolidone (PVP) K29/32 (Acros Organics, Belgium), gelatin (Merck, Germany), and pregelatinized starch 1500 (Colorcon, Germany), selected for regulatory acceptability and differing binding properties. Purified water served as the granulating solvent. Prolonged release (PR) granules were coated with Eudragit® RS 100 and RL 100 (Evonik, Germany) and plasticized with triethyl citrate (Merck, Germany), with talc as an anti-tacking agent and ethanol as the coating solvent. All materials were of Pharmacopeial or analytical grade and were used as received.

2.2. *Quality by design approach*

The development of MHCl granules was performed under the Quality by Design (QbD) framework, consistent with ICH Q8(R2) and Q9 guidelines.[9,11] The process involved defining the QTPP, identifying CQAs, and establishing links to CMAs and CPPs. Risk assessment included the use of Ishikawa (fishbone) diagrams to identify potential variability sources and FMECA to prioritize risks based on severity, probability, and detectability. This systematic approach guided binder selection, process optimization, and formulation robustness.

2.3. *Preparation of immediate-release granules*

Three immediate release (IR) formulations (F1–F3), each containing 500 mg of MHCl per dose, were prepared at a batch size of 100 g, differing only in binder type (PVP, gelatin, or pregelatinized starch 1500) (Table 1).

All ingredients were sieved (2.0 mm mesh), manually dry-blended in a mortar using a pestle, and manually granulated using 5% w/v aqueous binder solutions (corresponding to 2.5 g of binder in 50 g of purified water). For gelatin, the solution temperature was maintained at approximately 30 °C to ensure solubility. The binder solution was added at an approximate rate of 10 ml/min, ensuring uniform wetting of the powder mass without overwetting. Following binder addition, the wet mass was manually kneaded for 5 min per cycle to achieve a cohesive and uniformly wetted mass. This procedure was repeated five times, resulting in a total effective kneading time of 25 min. The wet mass was passed through a 2.0 mm sieve and dried in a tray oven at 50–60 °C for 60 min. The dried granules were re-sieved (2.0 mm mesh) and stored for evaluation.

T a b l e 1

Composition of metformin hydrochloride immediate-release granules

Ingredient (% (w/w))	Function	F1 IR	F2 IR	F3 IR
Metformin hydrochloride	API	50	50	50
Croscarmellose sodium	Superdisintegrant	2.5	2.5	2.5
Sodium starch glycolate	Superdisintegrant	5	5	5
Lactose monohydrate	Filler	27.25	27.25	27.25
Microcrystalline cellulose	Filler/Binder	10	10	10
Polyvinylpyrrolidone	Binder	2.5	–	–
Gelatin	Binder	–	2.5	–
Pregelatinized starch 1500	Binder	–	–	2.5
Sucrose	Sweetener	2	2	2
Talc	Lubricant/Glidant	0.75	0.75	0.75
Total	/	100	100	100

2.4. *Preparation of prolonged-release granules*

PR granules were prepared similarly to IR formulations but without disintegrants. These uncoated PR granules were designated as F1 PR-U, F2 PR-U, and F3 PR-U, respectively. After drying, granules retained between 1.4 and 2.0 mm were subjected to film coating in a laboratory-scale fluid-bed coater (Freund-Vector Corporation, USA) using a dispersion composed of: Eudragit® RS 100 (54 g), a water-insoluble low-permeability polymer forming film backbone; Eudragit® RL 100 (6 g), more permeable polymer that modulated film porosity and adjusted permeability; triethyl citrate (9 g) as plasticizer; talc (15 g) as anti-adherent; and ethanol (540 g) as solvent (formulations F1 PR, F2 PR, and F3 PR accordingly). The effective MHCl granules-to-total Eudragit ratio used for coating PR granules was 1:0.94 (±0.16), consistent with the typical variability expected in laboratory-scale fluid-bed processes. Key coating parameters were maintained as follows: inlet temperature 55–60 °C, product temperature 40–45 °C, atomization air pressure 500–600 mbar, airflow 150–160 l/min, and spray rate 5 rpm.

2.5. *Characterization of granules*

2.5.1. *Spectroscopic analysis (FTIR and Raman)*

Fourier transform infrared (FTIR) and Raman spectroscopy were used to assess potential interactions between MHCl and excipients during granulation and coating. FTIR spectra (Cary 600 FTIR spectrometer with diamond ATR accessory, Agilent Technologies, USA) were recorded over 4000–650 cm^{-1}. Raman spectra were acquired using an optical probe coupled to a portable Raman spectrometer (ATR3000-DH, Optosky, China), equipped with a 1064 nm excitation laser. Spectra were collected at a laser power of 400 mW, with a cumulative integration time of 60 s and an exposure time of 60 s.[12,13]

2.5.2. *Particle size and particle size distribution*

Particle size (PS) and particle size distribution (PSD) of the immediate-release (IR) (F1–F3 IR) and uncoated prolonged-release (PR-U) (F1–F3 PR-U) granules were determined by laser diffraction[14,15] using a Mastersizer 2000 equipped with a Scirocco 2000 dry powder feeder (Malvern, UK). PS was expressed as D_{50} ± SD, and PSD as the SPAN factor. Measurements were conducted at 2 bar pressure and 50 % feed rate, with obscuration maintained between 2 % and 3 %. The Mie optical model was applied, with particle refractive index (RI) of 1.52, absorption (Ai) of 0.1, and standard dispersant settings. Each sample was analyzed 3–5 times, and mean values were calculated.

For the PR granules (F1–F3 PR), laser diffraction was unsuitable due to their larger particle size. Instead, PS was determined by optical microscopy with image analysis using ImageJ software.[16] Additionally, the PS of formulations F1–F3 IR and F1–F3 PR-U was also measured using the same method. For each formulation, at least 1500 particles per sample (n = 3) were analyzed to obtain representative PS and PSD values.

2.5.3. *Granule morphology*

The morphology of IR and PR granules was evaluated by optical microscopy (Zeiss Axio Scope 5 with Axiocam 208 Color camera, Carl Zeiss Microscopy, Germany) under reflected-light and dark-field illumination at 25× magnification. Approximately 0.1 g of sample was spread on a microscope slide and scanned to obtain representative micrographs, which provided a qualitative assessment of granule shape and surface characteristics.[17,18]

Micrographs were analyzed using ImageJ software.[16] Images were converted to 8-bit grayscale, and the "Waviness and Roughness" plugin was applied with a 120-pixel cutoff to reduce background interference. Surface profile plots were generated, and the data (distance in pixels and gray value) were exported for analysis. The gray values were used to calculate the mean intensity and the arithmetic average roughness (Ra) (Eq. 1) as the mean absolute deviation from the overall mean gray value:

$$Ra = \frac{1}{N}\sum_{i=1}^{N} \quad | \, y_i - \bar{y} \, | \qquad (1)$$

where y_i is the gray value at point i, and $\bar{y}$ is the mean gray value.

The root-mean-square roughness (Rq) (Eq. 2) was calculated as the square root of the mean squared deviations from the mean:

$$Rq = \sqrt{\frac{1}{N}\sum_{i=1}^{N} \quad (y_i - \bar{y})^2} \qquad (2)$$

In this analysis, Rq corresponds numerically to the standard deviation of the gray-value distribution and provides information similar to R_a,[19] but with slightly greater sensitivity to higher peaks and deeper valleys. Together, these parameters together allow a quantitative comparison of surface

roughness among the different binder types and coating conditions.

2.5.4. *Moisture content (loss on drying)*

Residual moisture was determined using a halogen moisture analyzer (Mettler Toledo HB43-S, Switzerland).[20,21] Granules were analyzed after drying and re-sieving through a 2.0 mm mesh sieve. An accurately weighed sample of approximately 1.0 g was placed in the weighing pan, evenly distributed, and dried at 105 °C using the standard drying program until a constant mass was achieved, defined as a mass change not exceeding 1 mg over a 50 s interval. The measurements were performed in triplicate to ensure the reliability of the results. Moisture content values of ≤ 2.0% were targeted to maintain granule stability and flowability.

2.5.5. *Flow properties*

Bulk and tapped densities were determined in accordance with the European Pharmacopoeia (Ph. Eur.) 2.9.36.[22–25] A 100 g sample of each formulation (IR and PR) was placed into a 250 mL graduated cylinder and subjected to 1250 taps using a tap density tester (Erweka SVM 102, Germany). Carr's index (Eq. 3) and the Hausner ratio (Eq. 4) were subsequently calculated to evaluate granule flowability and packing characteristics, where ρb and ρt represents the bulk and tapped densities, respectively.

$$CI\ (\%) = \frac{\rho t - \rho b}{\rho t}\ x\ 100 \qquad (3)$$

$$Hausner\ ratio = \frac{\rho t}{\rho b} \qquad (4)$$

2.5.6. *Drug content*

Drug content of formulations F1–F3 IR and F1–F3 PR-U was determined by Ultraviolet-Visible (UV-Vis) spectrophotometry (Agilent Cary 60 UV-Vis Spectrophotometer, Agilent Technologies, USA) at 230 nm. Calibration standards (1–15 µg/mL) were prepared in purified water in triplicate to obtain a linear calibration curve. For analysis, 200 mg of granules were dissolved in 100 mL purified water, filtered through a 0.45 µm regenerated cellulose (RC) membrane filter, and appropriately diluted (to approximately 10 µg/mL MHCl) prior to measurement.

For coated PR formulations (F1–F3 PR), the MHCl assay was performed using HPLC (Agilent 1290 Infinity III LC System, USA) with detection at 230 nm. Quantification was based on the peak area ratio relative to a standard solution (0.05 mg/mL) prepared in diluent (water and acetonitrile (Merck, Germany) (90:10 v/v)). For sample preparation, 2 g of granules was dispersed in 100 mL of acetonitrile and sonicated (15 min, degassing mode). After adding approximately 200 mL of purified water, the mixture was stirred for 45 min, diluted to 500 mL with purified water, and manually shaken for 1 min to ensure homogeneity. The solution was centrifuged (2500 rpm, 10 min); 5.0 mL of the clear supernatant was diluted to 100 mL with diluent and filtered through a 0.45 µm RC membrane (the first 5 mL discarded), yielding a final concentration of 0.05 mg/mL. Separation was achieved on a Sun Fire C8 column (Waters, USA) (150 × 4.6 mm, 5 µm) at 25 °C, using a mobile phase consisting of phosphate buffer (pH 3.0) and acetonitrile (95:5, v/v) at a flow rate of 1.0 mL/min. The phosphate buffer was prepared by dissolving 2.76 g sodium dihydrogen phosphate monohydrate (Merck, Germany) and 0.871 g sodium 1-pentanesulfonate (Merck, Germany) in 800 mL water, adjusting pH to 3.0 with diluted orthophosphoric acid (Merck, Germany) (11.5% w/w H_3PO_4 in water), and diluting to 1000 mL, followed by filtration through a 0.20 µm membrane filter. The injection volume was 10 µL, and the total run time was 5 min. Drug content was assessed on at least three samples per formulation and expressed as mean ± SD (standard deviation).

2.5.7. *Drug release*

Dissolution testing of formulations F1–F3 IR and F1–F3 PR-U was performed using dissolution testing USP Apparatus I (rotation basket) at 100 rpm (Erweka DZT, Germany). One gram of granules was placed in 900 mL phosphate buffer (pH 6.8, 37 ± 0.5 °C) prepared according to Ph. Eur. 4.1.3[26] by mixing 51.0 mL of a 27.2 g/L solution of potassium dihydrogen phosphate (Merck, Germany) with 49.0 mL of a 71.6 g/L solution of disodium hydrogen phosphate (Merck, Germany), adjusting the pH if necessary. Samples (10 mL) were withdrawn at 5, 10, 15, 20, 30, and 45 min and replaced with fresh dissolution medium. After filtration through a 0.45 µm membrane filter, samples were analyzed by UV/Vis spectrophotometry (Agilent Cary 60, USA) at 230 nm. Tests were conducted in triplicate, and results are expressed as mean cumulative drug release (%) ± SD.

For PR formulations, 2 g of coated granules was tested in 1000 mL of phosphate buffer (pH 6.8, 37 ± 0.5 °C). Samples (10 mL) were collected at 1, 2, 3, 4, 5, 6, 7, 8, 10, 12, 14, and 24 h, with preheated medium replenished after each withdrawal. Filtered samples (0.45 μm) were analyzed by HPLC (Agilent 1290 Infinity III LC System, USA) at 230 nm. Dissolved MHCl (%) was calculated from peak area ratios relative to a standard solution. All tests were performed in triplicate and reported as mean cumulative release (%) ± SD.

2.5.8. *Statistical analysis*

Homogeneity of variances was assessed using Levene's test.[27] Depending on the results, either Welch's ANOVA (when homogeneity was violated, $p < 0.05$) or standard one-way ANOVA (when homogeneity was satisfied, $p > 0.05$) was applied, followed by appropriate post hoc tests (Games–Howell or Tukey, respectively).[27] Statistical significance was set at $p < 0.05$.

3. RESULTS AND DISCUSSION

3.1. *Quality target product profile*

The Quality Target Product Profile (QTPP) (Table S1, Supplementary Material) guided the development of IR and PR MHCl granules to meet the intended clinical performance. Both were designed as oral granules for direct use or reconstitution, enabling flexible dosing and improved acceptability in patients with swallowing difficulties.[28] A 500 mg dose was selected. The IR granules targeted a rapid release (≥ 80% within 45 min), while the PR granules aimed for a 24 h prolonged release. Key physical attributes ensured manufacturability and consistent performance: D_{50} of 0.5–1.5 mm (IR) and 2–3 mm (PR), as well as SPAN factor of ≤ 2.0 for flow, dose uniformity, and predictable dissolution. The granules were white to off-white, free-flowing, and had a moisture content of ≤ 2.0%. Quality attributes aligned with regulatory expectations: assay 95–105%, content uniformity a relative standard deviation (RSD) of ≤ 5%, and dissolution profiles matching the targeted release profiles. Microbiological limits followed Ph. Eur. standards[29] (total aerobic microbial count (TAMC), total yeast and mold count (TYMC), absence of *Escherichia coli*). Packaging in moisture- and light-protective unit-dose sachets or hard gelatin capsules was selected to maintain stability and usability. This QTPP provided the basis for identifying CQAs, risk assessment, formulation optimization, and process design within the QbD framework.

3.2. *Critical quality attributes*

Critical Quality Attributes (CQAs) are physical, chemical, biological, or microbiological attributes that must remain within defined limits to ensure compliance with the QTPP (ICH Q8(R2) and ICH Q9.[9,11] The identified CQAs (Table S2, Supplementary Material) ensured that both IR and PR MHCl granules met the clinical performance and stability requirements. Assay (95–105%) and content uniformity (RSD ≤ 5%) were critical for accurate dosing and a consistent therapeutic effect. Moisture content (≤ 2.0%) was critical due to its impact on chemical stability, dissolution, and microbial quality, especially for the hygroscopic MHCl. PS and PSD were CQAs for IR (D_{50}: 0.5–1 mm; SPAN factor ≤ 2) and PR granules (D_{50}: 2–3 mm; SPAN factor ≤ 2), affecting flow, uniformity, and dissolution. Dissolution was a key performance attribute: the IR granules required ≥ 80% release within 45 min, whereas the PR granules targeted a 24 h controlled release. Granule integrity was critical only for the PR granules; the IR granules required rapid disintegration. Microbial quality followed Ph. Eur. standards.[29] Flow properties (Carr's index ≤ 15%; Hausner ratio ≤ 1.18) was monitored but not classified as a CQA unless they impacted uniformity or dissolution. This CQA identification guided formulation optimization and risk-based process control in the QbD framework.

3.3. *Critical material attributes*

Critical Material Attributes (CMAs) are physicochemical or biological properties of the active pharmaceutical ingredient (API) and excipients that influence product CQAs. Identifying and controlling CMAs within the QbD framework enables mechanistic understanding of granule formation, drug release, and performance.[9,11] MHCl poses challenges due to its high solubility (> 300 mg/ml), hygroscopicity, and poor compressibility,[30] requiring careful excipient selection for the development of robust granules and reproducible release. The composition of the IR granules was intentionally designed to balance rapid disintegration, granule cohesion, and processability, with excipients selected through a function-driven approach to meet the required performance. Key CMAs (Table S3, Supplementary Material) include API PS and PSD, hygroscopicity, and bulk density, which affect uniformity, moisture

sensitivity, and flow. Binder type and concentration (PVP, gelatin, pregelatinized starch 1500) govern granule cohesion and dissolution, requiring optimization for both IR and PR systems.[31]

The IR granules rely on disintegrants (croscarmellose sodium and sodium starch glycolate) for rapid release. These disintegrants were used together to combine complementary mechanisms: croscarmellose sodium rapidly draws water into the granule via capillary channels and swelling multidirectionally to initiate disintegration, while sodium starch glycolate absorbs water and swells extensively (up to 7–8 times its volume), physically disrupting the matrix. Together, these mechanisms ensure rapid and reliable granule disintegration.[32,33] The PR formulations depend on Eudragit® coating properties for sustained release. Fillers (α-lactose monohydrate and microcrystalline cellulose) improve bulk and flow but may affect moisture uptake. Talc serves as a lubricant and anti-adherent, enhancing manufacturability but potentially retarding dissolution at high levels. Sucrose functions as a binder, diluent, and mild sweetener in wet granulation, improving agglomeration and palatability of the bitter MHCl without significantly affecting release. The low levels used comply with European Union guidance (approximately 5 g per dose), ensuring negligible sugar exposure.[34] The quantity of purified water is also critical, as over-wetting may cause agglomeration or pose a microbial risk. The most formulation-sensitive CMAs, API PS/PSD, binder, disintegrant, and polymer film properties, strongly impact moisture content, granule integrity, and dissolution, supporting consistent IR and PR quality.[35]

3.4. *Critical process parameters*

Critical Process Parameters (CPPs) are measurable and controllable process variables that directly affect CQAs, ensuring consistent compliance with the QTPP.[9,11] For MHCl granules, CPPs were identified across weighing, binder preparation, wet granulation, sieving, drying, and coating (PR only) using prior knowledge, preliminary trials, and risk assessment (Table S4, Supplementary Material). For IR granules, the critical parameters include the binder addition rate, kneading time, drying temperature, and resulting PS and PSD, which govern granule cohesion, disintegration, and rapid dissolution. For the PR granules, the coating parameters, spray rate, atomization pressure, and inlet air temperature, ensure uniform polymer films and reproducible prolonged release. Overall, the manufacturing of MHCl granules is sensitive to material handling and process conditions. Controlling CPPs within a defined design space reduces variability in moisture content, granule integrity, and dissolution, supporting consistent IR and PR quality. A systematic CPP–CQA evaluation underpins a science-based control strategy, enhancing process robustness and scalability.[36]

3.5. *Risk assessment*

Risk assessment is a cornerstone of the QbD framework, providing a structured, science-based approach to identify, evaluate, and mitigate factors that may impact product quality.[9,11] In this study, a dual strategy combining qualitative Ishikawa (fishbone) analysis and semi-quantitative Failure Mode, Effects, and Criticality Analysis (FMECA) was applied to both IR and PR MHCl granules. This integrated approach enabled the systematic identification of critical risks and guided the development of robust control strategies.

3.5.1. *Ishikawa analysis*

Separate Ishikawa (fishbone) diagrams were developed for IR and PR MHCl granules to reflect the distinct formulation goals of each. For the IR granules, material-related risks included API hygroscopicity, binder variability, and disintegrant performance, while method-related risks involved binder solution preparation, granulation endpoint, and drying uniformity (Fig. S1, Supplementary Material). Equipment-, operator-, and environmental-related factors (oven temperature, kneading, sieving, humidity, and contamination) were also considered. For the PR granules, additional risks arose from fluid-bed coating. Material-related risks included binder strength, polymer dispersion stability, and plasticizer/solvent compatibility (Fig. S2, Supplementary Material). Process-related risks covered granulation consistency, drying, and coating parameters (spray rate, atomization pressure, inlet/outlet temperatures). Equipment-, operator-, and environmental-related factors (nozzle clogging, airflow, sensors, operator skill, humidity, ventilation, and light exposure) were critical for coating quality and polymer stability.

3.5.2. *Failure mode, effects and criticality analysis*

Failure Mode, Effects, and Criticality Analysis (FMECA) quantitatively assessed risks by scoring Severity (S), Occurrence (O), and Detectability (D) on a 1–5 scale, with Risk Priority Number (RPN = S × O × D) ranging up to 125 (Fig. S3,

Supplementary Material).[11,37] Higher RPNs indicated risks requiring mitigation.

For IR MHCl granules, the highest risks were binder performance (RPN = 24), API hygroscopicity, disintegrant performance, and operator variability (RPN up to 18), all of which affect disintegration and dissolution. These findings highlighted the need for robust standard operating procedures (SOPs), monitoring, and training.

In PR MHCl granules, fluid-bed coating was the most critical step (RPN = 30), being sensitive to nozzle performance, spray rate, airflow, and temperature. API hygroscopicity (RPN = 24) could increase moisture content, cause caking, reduce flow, and affect dissolution. Binder performance was also critical for granule cohesion, mechanical strength, and the sustained-release integrity (RPN = 24). These findings are consistent with literature reports indicating that for highly soluble substances, the binder solution has a dominant influence on granule growth kinetics compared to other process factors.[38]

High-risk steps were controlled via process monitoring, humidity management, protective packaging, and in-process testing (loss on drying, dissolution, and flow). FMECA identified binder preparation and hydration, granulation, drying, and coating as the most sensitive aspects, requiring continuous control to ensure consistent quality and QTPP compliance for both IR and PR MHCl granules (Table S5, Supplementary Material).

3.6. *Preparation of granules*

Manual wet granulation was employed as a small-scale, controlled laboratory method, allowing precise adjustment of the wet massing endpoint, which is critical for achieving reproducible granule properties, particularly for formulations intended for coating. For highly soluble drugs such as MHCl, this approach is particularly important, as it enables identification of the narrow "solubility window," where slight variations in liquid addition can significantly affect granule formation.

Following the risk assessment, three prototype IR and PR MHCl formulations, each with a different binder, were prepared and evaluated for key CQAs: moisture content, flow, PS and PSD, assay, and dissolution, all consistent with the QbD approach. The IR granules targeted rapid disintegration and ≥ 80% release within 45 min, while PR granules aimed for 24 h sustained release. FTIR and Raman spectroscopy confirmed the absence of API–excipient interactions. This stage verified high-risk variables, especially binder type, and provided data to optimize granule robustness, flow, and release profiles in line with the QTPP.

3.7. *Characterization of granules*

3.7.1. *Spectroscopic analysis (FTIR and Raman)*

The Fourier transform infrared (FTIR) spectrum of MHCl (Fig. 1a) showed a broad N–H stretching band at approximately 3365 cm^{-1} and 3145 cm^{-1}, a strong C=N stretch at 1622 cm^{-1}, an N–H bending/C–N stretch at 1559 cm^{-1}, and CH_3 deformation bands at 1473–1445 cm^{-1}. C–N stretching bands appeared at 1289 cm^{-1}, 1270 cm^{-1}, and 1207 cm^{-1}, with additional aliphatic C–N bands at 1059 cm^{-1} and 1037 cm^{-1}, and N–C–N skeletal vibration bands at 935 cm^{-1}.[39]

The FTIR spectrum of α-lactose monohydrate (Fig. 1b) displayed a broad O–H stretching at 3400–3200 cm^{-1}, an aliphatic C–H at approximately 2989 cm^{-1}, CH_2 scissoring and C–H bending at 1421 cm^{-1} and 1380 cm^{-1}, and strong C–O–C/C–O stretching bands at 1140 cm^{-1}, 1083 cm^{-1}, 1057 cm^{-1}, and 1041–1018 cm^{-1}. Bands at 914 cm^{-1}, 751 cm^{-1}, and 674 cm^{-1} corresponded to ring and skeletal vibrations.[40]

The FTIR spectra of IR MHCl granules (Fig. 1c–e) showed the characteristic features of both MHCl and α-lactose monohydrate, with no new bands or significant shifts, indicating a physical mixture without chemical interaction or degradation. Minor O–H/N–H band broadening was observed, likely arising from hydrogen bonding during wet granulation.

The FTIR spectra of Eudragit® RL100 and Eudragit® RS100 (Fig. 1f-g) exhibited a prominent ester carbonyl (C=O) stretching band at approximately 1721 cm^{-1}, aliphatic C–H stretching bands at 2950–2850 cm^{-1}, CH_2/CH_3 deformation bands at approximately 1441 cm^{-1}, and C–O/C–O–C stretching bands at 1234 cm^{-1}, 1189 cm^{-1}, and 1100–1050 cm^{-1}. A band at approximately 751 cm^{-1} was observed to correspond to skeletal/C–C–O deformation vibrations.

In the coated PR MHCl granules (Fig. 1h–j), the polymer's characteristic bands dominated, especially the carbonyl (C=O) and C–O–C stretching bands, which overlapped the MHCl signals. No new bands or significant shifts were observed, indicating an absence of chemical interaction. The ATR-FTIR profile confirmed a continuous Eudragit® coating that was consistent with an intact polymer layer capable of controlling MHCl release.

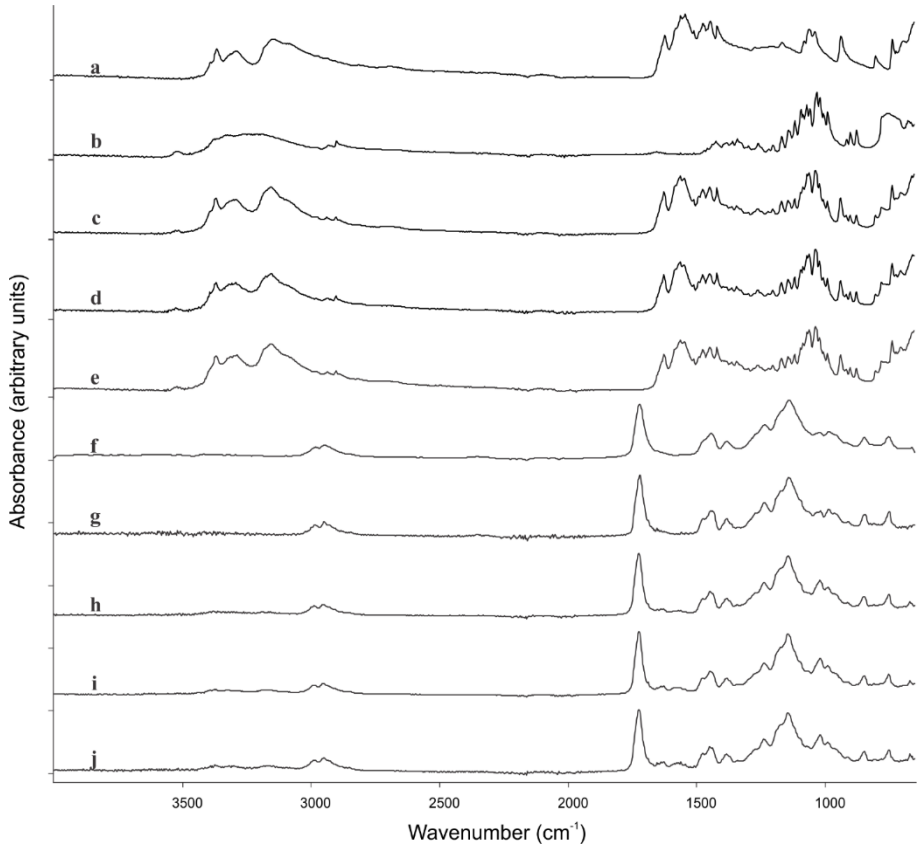

Fig. 1. FTIR spectra of: (a) metformin hydrochloride, (b) α-lactose monohydrate, (c) F1 IR, (d) F2 IR, (e) F3 IR, (f) Eudragit® RL100, (g) Eudragit® RS100, (h) F1 PR, (i) F2 PR, and (j) F3 PR.

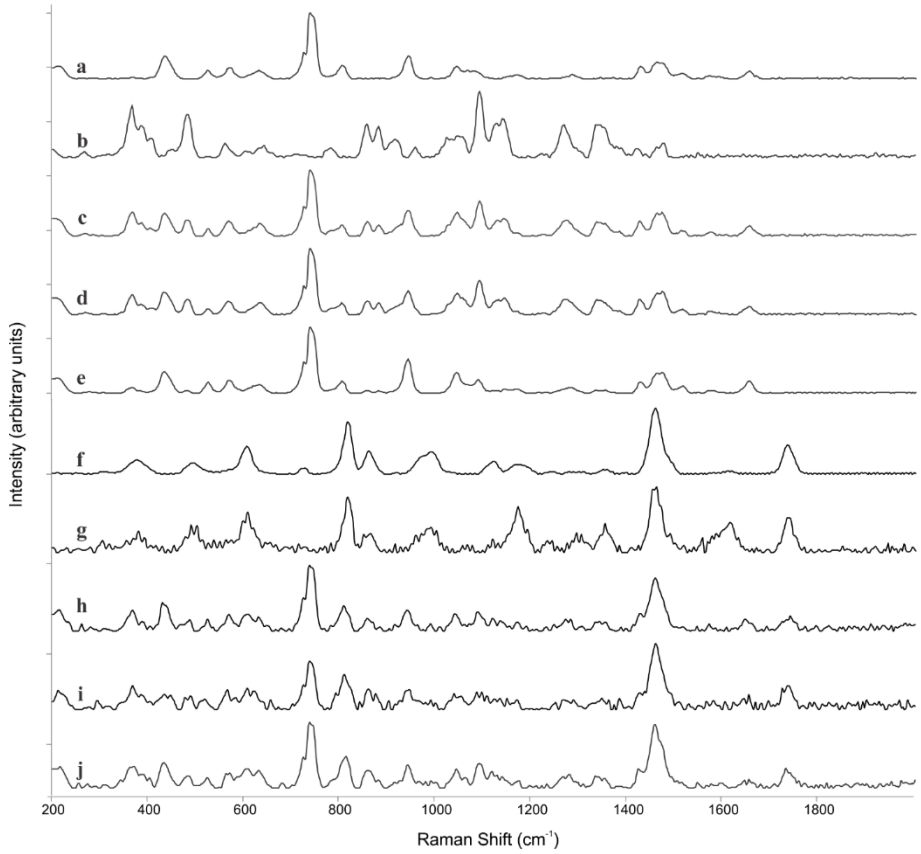

Fig. 2. Raman spectra of: (a) metformin hydrochloride, (b) α-lactose monohydrate, (c) F1 IR, (d) F2 IR, (e) F3 IR, (f) Eudragit® RL100, (g) Eudragit® RS100, (h) F1 PR, (i) F2 PR, and (j) F3 PR.

The Raman spectrum of MHCl (Fig. 2a) showed key bands at 430 cm^{-1} (C–N–C deformation), 774 cm^{-1} (biguanide C–N–C stretching), 937 cm^{-1} (C–N skeletal vibration), 1423/1458 cm^{-1} (CH_3 deformation), and 1651 cm^{-1} (C=N stretching).[41]

α-Lactose monohydrate (Fig. 2b) exhibited bands at 862–876 cm^{-1} (C–H and ring modes), 1089 cm^{-1} (C–O stretching), 1124–1136 cm^{-1} (C–O–C stretching), 1416/1448 cm^{-1} (CH_2/CH deformation), and lattice modes at 382 and 478 cm^{-1}, which confirmed the crystallinity.[40]

The Raman spectra of IR MHCl granules (Fig. 2c–e) showed features of both MHCl and α-lactose monohydrate, which were dominated by the MHCl signals with no peak shifts, indicating an absence of chemical changes or solid-state interactions during wet granulation.

The Raman spectra of Eudragit® RL100 and Eudragit® RS100 spectra (Fig. 2f–g) were marked by the ester carbonyl (C=O) stretching band at approximately 1731 cm^{-1}, CH_2/CH_3 deformation bands at 1454 cm^{-1}, and C–C–O/C–O–C stretching bands at 811 and 1117–1171 cm^{-1}. These features dominated the spectra of the coated PR MHCl granules (F1–F3 PR, Fig. 2h–j), though the MHCl 774 cm^{-1} band remained detectable due to partial laser penetration through the thin polymer layer. This result contrasted with the data obtained from ATR-FTIR spectroscopy, where the signal was reflected from the sample surface only, with a probing depth of 1-2 μm.

3.7.2. *Particle size and particle size distribution*

The binder type influenced the granule particle size across all formulations (Table 2; PSD profiles are shown in Fig. 3 (IR and PR-U granules) and Fig. 4 (for the PR granules)). Laser diffraction analysis of the IR granules (F1–F3 IR) showed clear binder-dependent differences (Fig. 3a): the F1 IR (PVP) formulation formed the largest, most cohesive granules; the F3 IR (pregelatinized starch 1500) formulation exhibited an intermediate size; and F2 IR (gelatin) formulation produced the smallest granules, reflecting differences in the binder properties.

The PVP-based IR granules (F1 IR) exhibited the largest median particle size and the narrowest PSD, reflecting strong wetting and cohesion during granulation. PVP rapidly dissolves and forms hydrogen bonds via its lactam carbonyl groups, promoting solid bridge formation, which is consistent with previous wet- or fluid-bed granulation studies.[42,43] The gelatin granules (F2 IR) had a smaller D_{50} and a broader PSD due to temperature-dependent gelation and heterogeneous binder distribution, which produced variable internal density.[44] Pregelatinized starch 1500 (F3 IR) yielded intermediate particle sizes with high surface roughness and residual moisture, reflecting its amorphous, water-absorbing structure, which increases granule porosity and affects hydration and dissolution.[45] The PR-U granules prepared without a disintegrant (Fig. 3c) showed similar PSDs (1.4–2.0 mm), indicating minimal disintegrant effect.

T a b l e 2

Particle size (PS), particle size distribution (PSD), and SPAN values for IR, PR-U, and PR granules (n = 3–5)

Formulation	D10	D50	D90	SPAN	Method
F1 IR (PVP)	608.8 ± 170.3 μm	995.2 ± 97.8 μm	1487.9 ± 30.8 μm	0.878 ± 0.24	Laser diffraction
	489.5 ± 19.5μm	774 ± 30.9 μm	1667.7 ± 80 μm	1.52 ± 0.14	Optical microscopy + ImageJ
F2 IR (Gelatin)	239.2 ± 12.4 μm	631.8 ± 14.6 μm	1271.9 ± 10.7 μm	1.635 ± 0.041	Laser diffraction
	479.5 ± 9.3 μm	758.2 ± 14.6 μm	1752.3 ± 17.9 μm	1.68 ± 0.48	Optical microscopy + ImageJ
F3 IR (Pregelatinized starch 1500)	464.6 ± 196.4 μm	858.2 ± 207 μm	1437.6 ± 164.6 μm	1.266 ± 0.422	Laser diffraction
	486.4 ± 11.4 μm	818.5 ± 83.3 μm	1822.2 ± 85.5μm	1.63 ± 0.12	Optical microscopy + ImageJ
F1 PR-U	632.4 ± 9.4 μm	1043.8 ± 20.1 μm	1577.6 ± 40.7 μm	0.908 ± 0.02	Laser diffraction
	485 ± 10.5 μm	766.9 ± 16.63 μm	1533.7 ± 33.2 μm	1.37 ± 0.002	Optical microscopy + ImageJ
F2 PR-U	675.8 ± 39.81 μm	1071.6 ± 21.1 μm	1596.6 ± 8.5 μm	0.859 ± 0.06	Laser diffraction
	488.2 ± 5.3 μm	771.8 ± 8.4 μm	1770.3 ± 90.2 μm	1.66 ± 0.0.09	Optical microscopy + ImageJ
F3 PR-U	634.6 ± 4.2μm	1041.7 ± 17μm	1591.8 ± 17.2 μm	0.920 ± 0.006	Laser diffraction
	488.1 ± 4.92 μm	771.8 ± 7.73 μm	1725.7 ± 17.56μm	1.6 ± 0.003	Optical microscopy + ImageJ
F1 PR	1.07 ± 0.14 mm	1.92 ± 0.03 mm	3.72 ± 0.4 mm	1.380 ± 0.2	Optical microscopy + ImageJ
F2 PR	1.26 ± 0.07 mm	2.08 ± 0.12 mm	3.82 ± 0.17 mm	1.230 ± 0.07	Optical microscopy + ImageJ
F3 PR	1.20 ± 0.06mm	2.01 ± 0.12 mm	3.55 ± 0.15 mm	1.170 ± 0.11	Optical microscopy + ImageJ

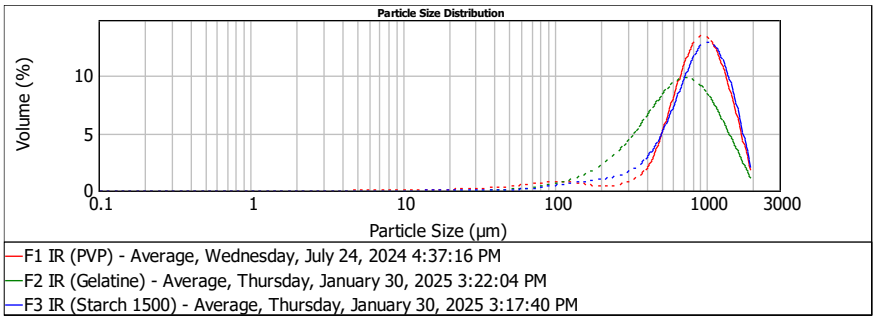

(a)

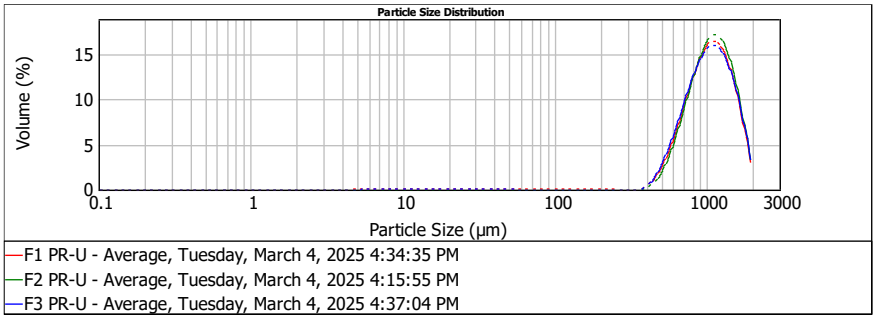

(b)

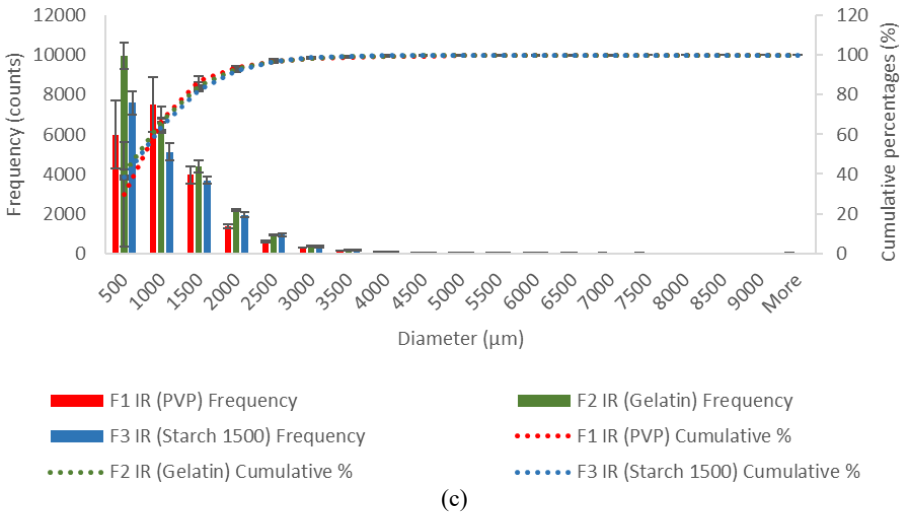

(c)

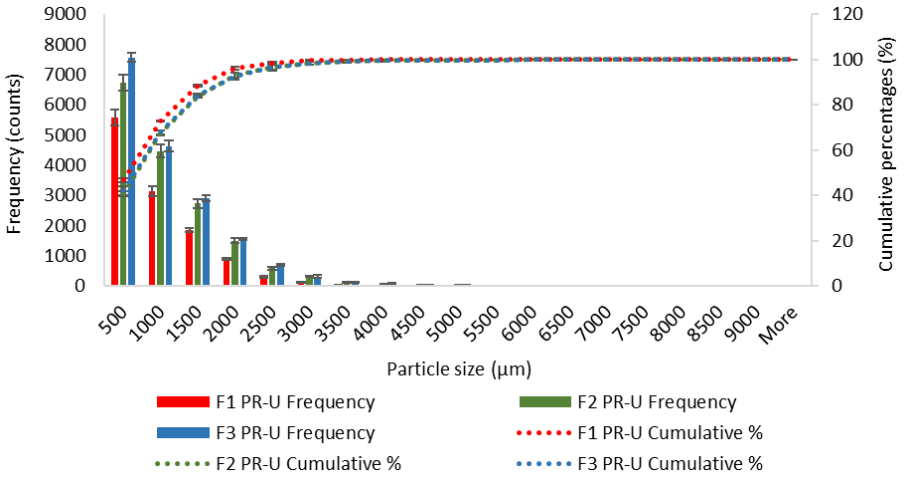

(d)

Fig. 3. Particle size and particle size distribution of metformin hydrochloride granules. Laser diffraction analysis: (a) IR granules and (b) PR-U granules (n = 3–5). Optical microscopy with ImageJ analysis: (c) IR and (d) PR-U granules. Data are presented as mean ± SD (n = 3–4). In cases where the SD bars are not visible, the data markers exceed the size of the error bars.

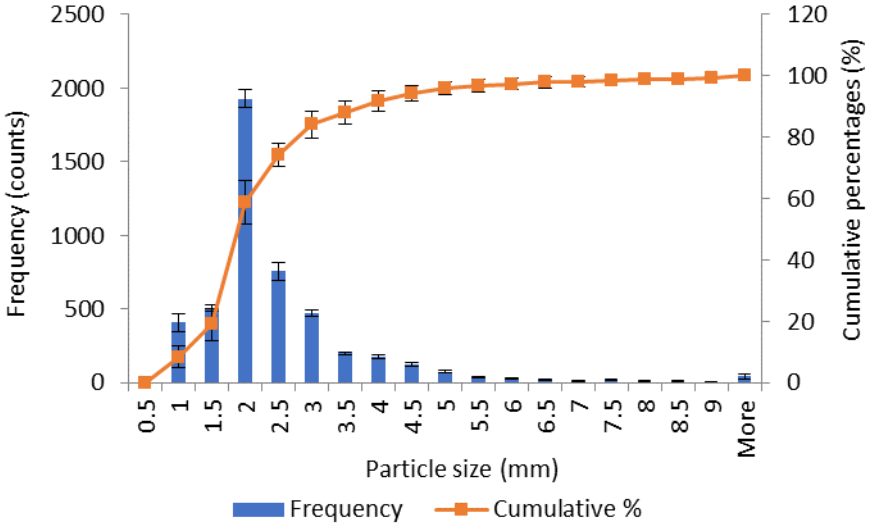

(a)

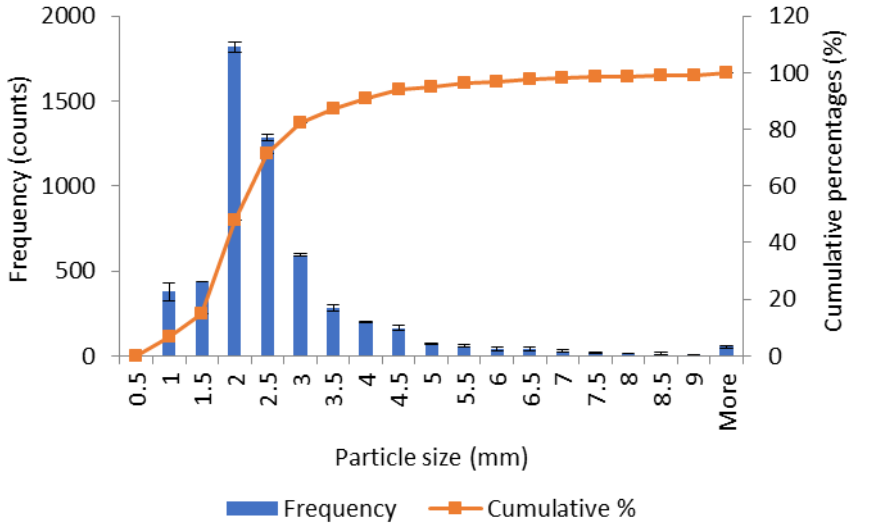

(b)

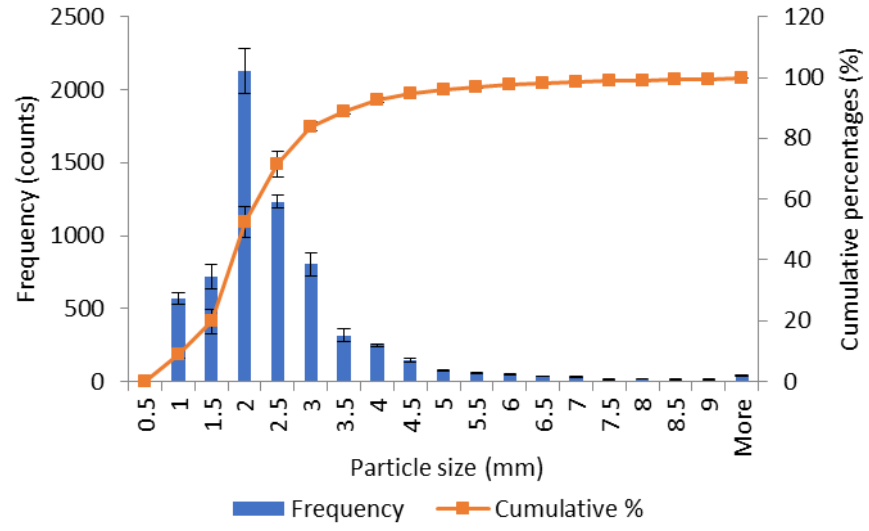

(c)

Fig. 4. PS and PSD histograms of PR granules obtained via optical microscopy and ImageJ analysis: (a) F1 PR, (b) F2 PR, and (c) F3 PR. Data are presented as mean ± SD (n = 3). In cases where the SD bars are not visible, the data markers exceed the size of the error bars.

Comparison with optical microscopy (ImageJ) (Table 2, Figs. 3b, 3d) showed method-dependent differences in absolute values. ImageJ generally yielded lower D_{50} values for F1 IR and all PR-U formulations (≈ 20–30% lower), while F3 IR showed good agreement between methods. An exception was observed for F2 IR (gelatin), where ImageJ produced a higher D_{50}, consistent with its broader distribution (similar SPAN values were obtained using both methods), suggesting a more heterogeneous particle population. In addition, SPAN values were slightly higher for ImageJ (≈ 1.3–1.7) than for laser diffraction (≈ 0.86–1.64), reflecting broader number-based distributions. However, all values remained below 2, indicating that, overall, the formulations exhibited predominantly unimodal particle size distributions, which is generally considered acceptable in pharmaceutical systems. It should be noted that granule shapes were not perfectly spherical (Figs. 5 and 6), which limited direct comparison between number-based ImageJ data and volume-based laser diffraction measurements. Nevertheless, laser diffraction provided a rapid and reproducible assessment of particle size distributions for all formulations, capturing the volume-weighted characteristics that were most relevant for downstream processing and dosage form performance. Despite method-dependent differences, the overall size ranges and granulation trends observed were consistent and reliable.

PR granules (F1–F3 PR) were larger and were analyzed by optical microscopy with ImageJ. The resulting PSD histograms are shown in Fig. 4, and PS parameters are listed in Table 2. F2 PR exhibited the narrowest, most uniform size distribution (lowest SPAN), while F1 PR showed the broadest. All PR granules were substantially larger than the IR granules, confirming successful coating and prolonged-release granulation.

3.7.3. *Granule morphology*

Optical micrographs of the PR-U granules revealed distinct morphologies (Fig. 5). F1 PR-U granules exhibited irregular but moderately rough surfaces, F2 PR-U granules displayed more pronounced surface irregularities and asymmetry, and F3 PR-U granules were highly irregular with a heterogeneous texture, reflecting binder distribution and granulation variability. These differences could have affected flow, compressibility, and drug release. The Eudragit® RS/RL coating (Fig. 6) produced irregular, near-spherical granules (2.4–2.8 mm) with compact, nodular surfaces, continuous and adherent films, and no visible cracks or core exposure, indicating good mechanical integrity. Surface roughness parameters (Ra, Rq, and mean gray value) are summarized in Table 3.

The binder type had a pronounced effect on the surface morphology of the uncoated granules. Among F1–F3 PR-U, starch-based F3 PR-U showed the highest roughness (Rq 29.81), followed by gelatin-based F2 PR-U, while PVP F1 PR-U displayed the smoothest surfaces (Ra 15.91, Rq 21.72), indicating a more uniform texture. Eudragit® coating (F1–F3 PR) reduced roughness across all formulations, most notably in gelatin F2 PR (Ra decreased by approximately 25%). PVP F1 PR remained the smoothest (Ra 14.47, Rq 19.59), whereas the coated starch F3 PR retained the highest roughness, suggesting that the polymer film only partially masked the irregular underlying structure.

These results clearly demonstrated that the binder type governed granule microstructure through its influence on liquid bridge formation, solid bridge consolidation, and post-drying hydration. Even at a constant binder concentration (2.5% w/w) and under identical wet-granulation conditions, PVP, gelatin, and pregelatinized starch 1500 produced granules with distinct particle size distributions, surface roughness, moisture retention, and dissolution behavior. These findings are consistent with the principle that, in high-drug-load systems, the binder is the primary excipient controlling granule integrity and internal porosity.[43,46] Overall, PVP produced the smoothest granules both before and after coating, gelatin exhibited intermediate properties, and starch led to the roughest surfaces, with Eudragit® coating improving smoothness most effectively for the gelatin granules.

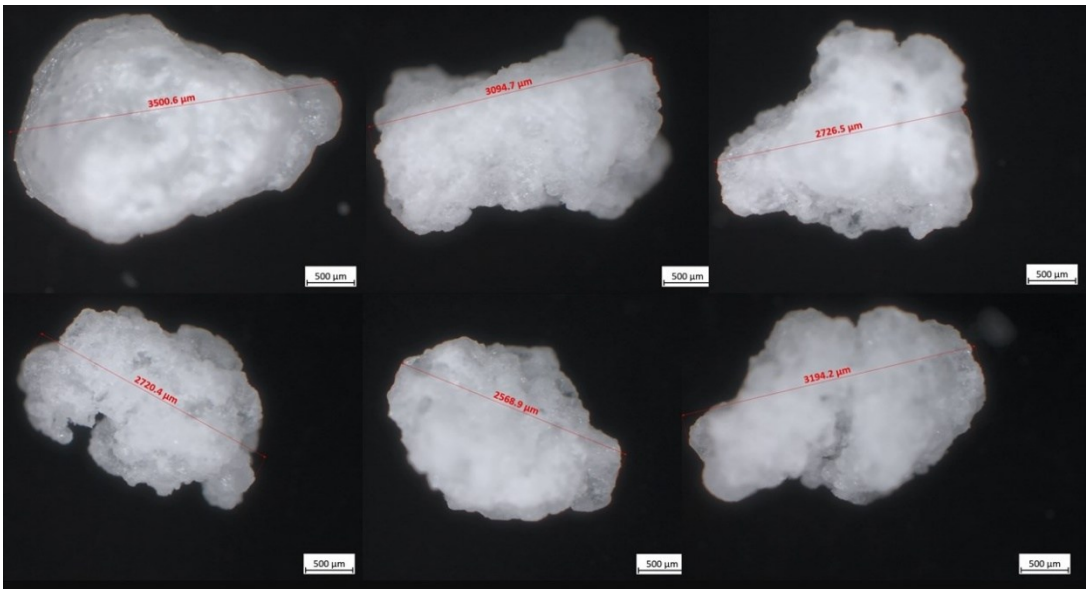

(a)

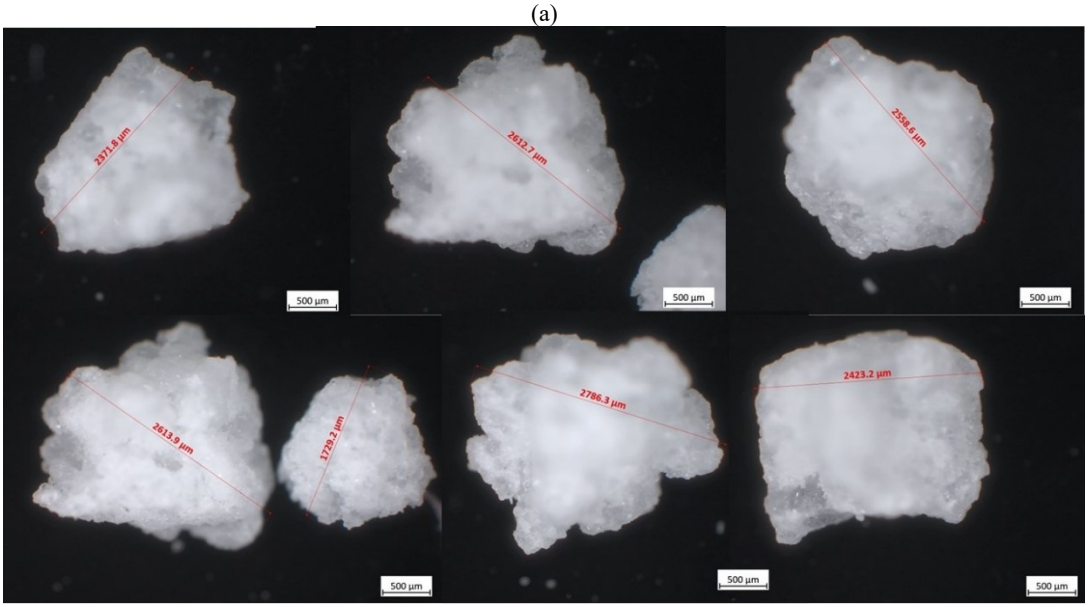

(b)

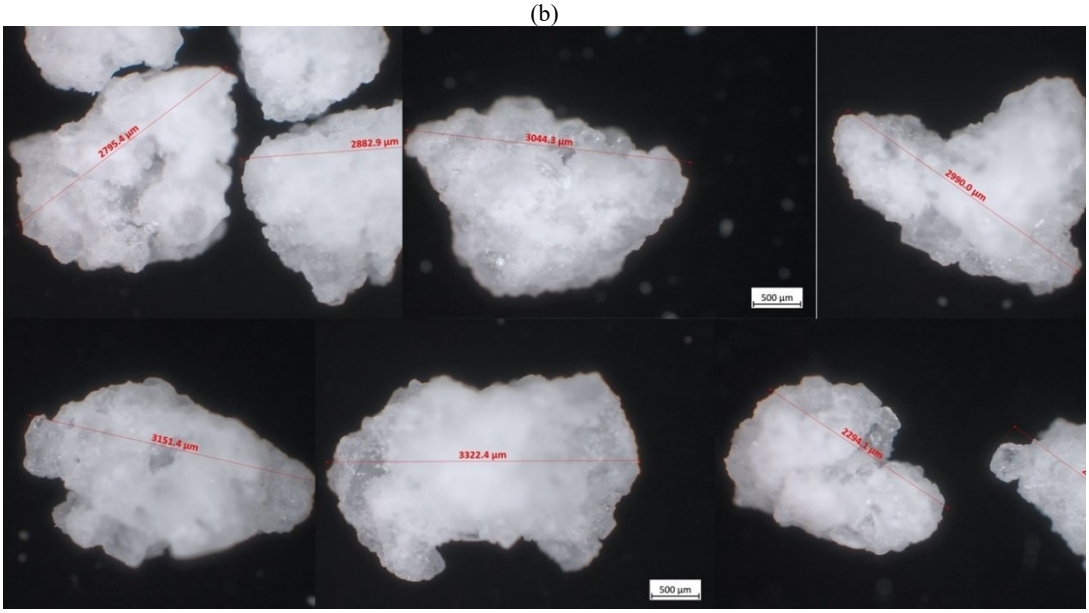

(c)

Fig. 5. Optical micrographs of metformin hydrochloride PR-U granules: (a) F1 PR-U, (b) F2 PR-U, and (c) F3 PR-U

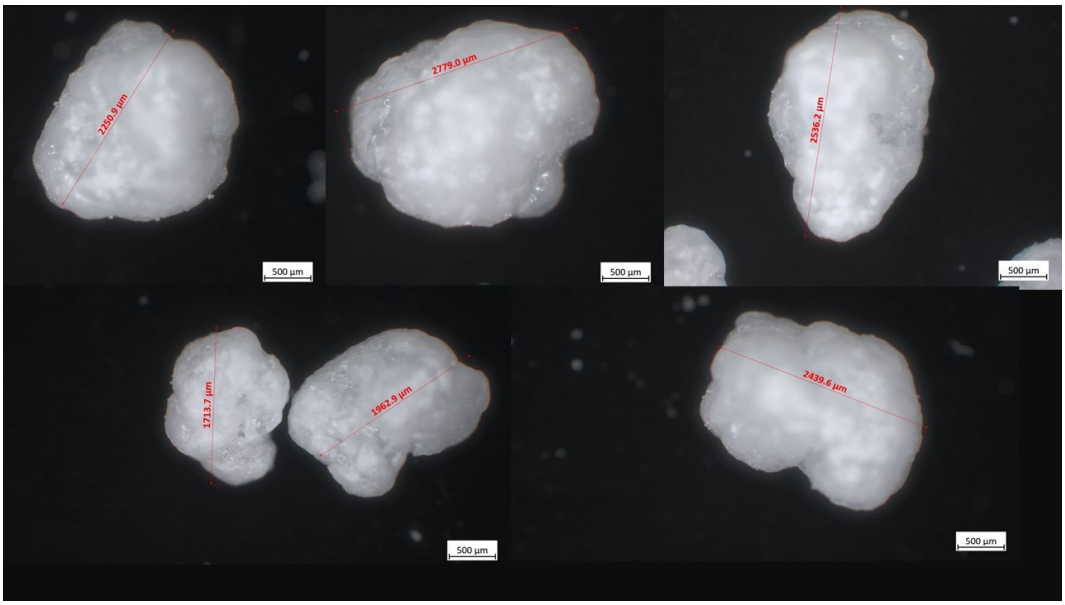

(a)

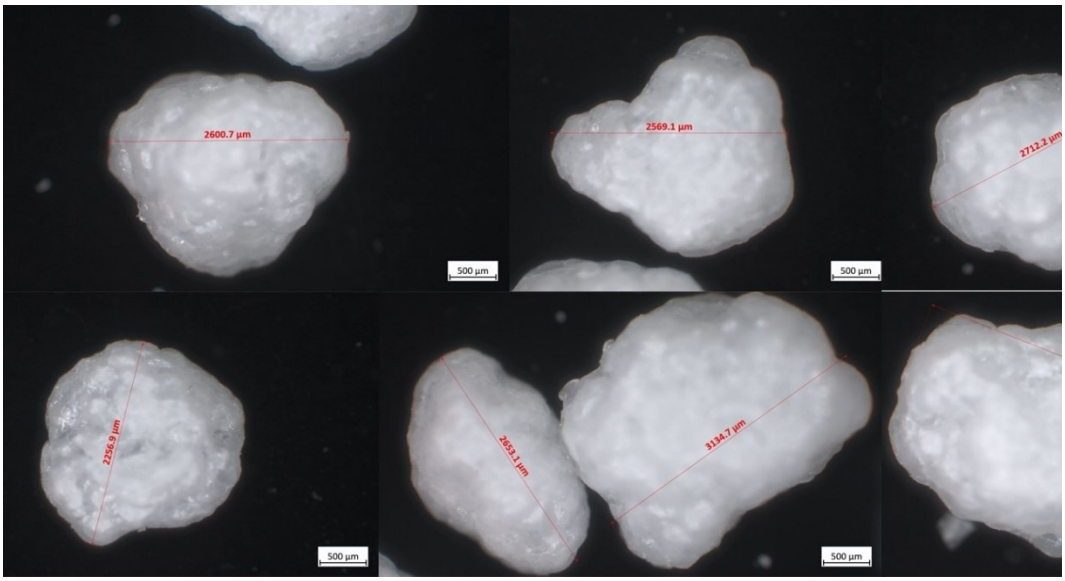

(b)

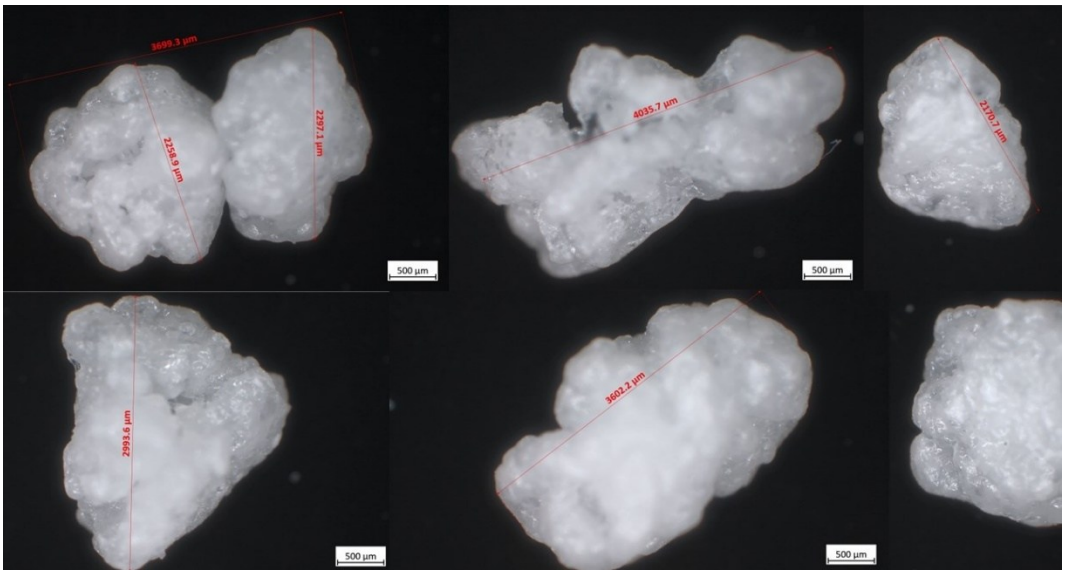

(c)

Fig. 6. Optical micrographs of metformin hydrochloride PR granules (a) F1 PR, (b) F2 PR, and (c) F3 PR

T a b l e 3

Effect of binder type and Eudragit® coating on surface roughness parameters of granules, as determined by ImageJ analysis

	Mean gray value	Ra (Arithmetic average height deviation)	Rq (Root mean square roughness)
F1 PR-U	1.24	15.91	21.72
F2 PR-U	2.25	20.80	29.32
F3 PR-U	6.05	19.72	29.81
F1 PR	2.01	14.47	19.59
F2 PR	4.65	15.69	22.93
F3 PR	1.36	16.69	24.21

3.7.4. *Moisture content (loss on drying)*

F1 IR (PVP) and F2 IR (gelatin) exhibited low residual moisture (1.63 ± 0.04 % and 1.66 ± 0.06 %, respectively), which was below the 2.0% w/w. This finding is consistent with literature reports for metformin hydrochloride formulations, where granules are typically dried to approximately 2–3 % w/w prior to compression to ensure adequate flowability and suitability for further processing.[47] In contrast, F3 IR (pregelatinized starch 1500) retained higher moisture (2.68 ± 0.10 %) due to the hygroscopicity of the starch. The higher moisture content in the starch granules likely promoted faster water ingress during dissolution and reduced resistance to early drug release, whereas the PVP and gelatin granules maintained more stable structures. One-way ANOVA confirmed significant differences among formulations ($p < 0.05$), and the Tukey post hoc test demonstrated significant differences between F3 IR versus F1 IR and F3 IR versus F2 IR. These results highlight binder type and moisture content as high-impact CMAs for hygroscopic, highly soluble MHCl formulations.[48]

3.7.5. *Flow properties*

The bulk and tapped densities, along with flowability parameters, are summarized in Table 4. Among the IR granules, F2 IR (gelatin) exhibited slightly better flow properties than F1 IR (PVP) and F3 IR (Pregelatinized starch 1500), as reflected by its lower compressibility (Carr's index) and Hausner ratio. Statistical analysis (Welch's ANOVA with Games–Howell post hoc test) indicated that the differences between the IR granules were significant for F2 IR versus F3 IR for both the Carr's index and the Hausner ratio ($p < 0.05$). The PR-U granules, which were prepared without disintegrants or coatings, exhibited moderately higher cohesiveness compared to the IR granules but maintained acceptable flow characteristics overall. For PR-U granules (Welch's ANOVA with Games–Howell post hoc test), significant differences were observed between F1 PR-U versus F2 PR-U and F2 PR-U versus F3 PR-U for both the Carr's index and the Hausner ratio ($p < 0.05$).

The PR granules coated with Eudragit® RS/RL displayed the highest bulk and tapped densities and improved flowability, with very low Carr's indices and Hausner ratios near unity. These improvements were confirmed statistically, showing that the PR granules had significantly better flow than their IR and PR-U counterparts for both the Carr index and the Hausner ratio (Welch's ANOVA with Games–Howell post hoc test, $p < 0.05$), except for F2 IR versus F2 PR in the Hausner ratio; this exception was likely due to similar bulk-to-tapped density ratios despite differences in compressibility. This enhancement in flow was likely due to the successful application of the coating layer, which increased granule mass and smoothed particle surfaces, thereby reducing interparticle friction and promoting better packing. These results confirmed that the coating process produced mechanically robust granules. The slightly poorer flowability observed in F2 PR (gelatin-coated granules), despite acceptable Carr's index (3%) and Hausner ratio (1.03), could be explained by the morphological characteristics imparted by the gelatin coating. Gelatin tends to form a smoother, somewhat tacky surface layer that increases interparticle adhesion, especially under conditions of residual moisture. This layer can reduce the ease of particle rearrangement during tapping, thereby manifesting as marginally impaired flow compared to uncoated or starch-based systems. In contrast, F3 PR (pregelatinized starch 1500) showed higher moisture content but still demonstrated excellent flowability (Carr index 2%,

Hausner ratio 1.02). Statistical analysis indicated that, for PR granules, a significant difference was observed only for the Carr's index between F2 PR and F3 PR (Welch's ANOVA with Games–Howell post hoc test, $p < 0.05$). This difference was attributable to the morphology and particle size distribution of the pregelatinized starch, which typically yields larger, more irregular particles with porous surfaces. Such morphology reduces cohesive forces and enhances interlocking, allowing good packing and flow even in the presence of absorbed moisture. Thus, the differences in flow properties between F2 PR and F3 PR can be rationalized by surface morphology and particle size effects: the gelatin coating promotes smoother, more cohesive granules, while pregelatinized starch contributes to bulkier, less cohesive particles that maintain good flow despite hygroscopicity.[49]

T a b l e 4

Bulk and tapped density, Carr's index, and Hausner ratio of IR, PR-U, and coated PR granules

Formulation	Bulk density (g/ml)	Tapped density (g/ml)	Carr index (%)	Hausner ratio
F1 IR	0.516 ± 0.018	0.580 ± 0.023	11 ± 2.58	1.13 ± 0.031
F2 IR	0.488 ± 0.02	0.525 ± 0.025	7 ± 1.15	1.08 ± 0.017
F3 IR	0.596 ± 0.005	0.677 ± 0.005	12 ± 0.5	1.13 ± 0.01
F1 PR-U	0.511 ± 0.008	0.603 ± 0.009	15 ± 1	1.18 ± 0.006
F2 PR-U	0.559 ± 0.006	0.621 ± 0.007	10 ± 0.577	1.11 ± 0.006
F3 PR-U	0.506 ± 0.005	0.584 ± 0.005	13 ± 0.577	1.15 ± 0.006
F1 PR	0.710 ± 0.004	0.723 ± 0.004	2 ± 0.577	1.02 ± 0.006
F2 PR	0.674 ± 0.005	0.697 ± 0.003	3 ± 0	1.03 ± 0.006
F3 PR	0.646 ± 0.004	0.659 ± 0.003	2 ± 0	1.02 ± 0.006

3.7.6. *Drug content*

The MHCl content in the IR granules was as follows: F1 IR (PVP), 509.0 ± 25.2 mg/g; F2 IR (gelatin), 523.8 ± 24.5 mg/g; and F3 IR (Pregelatinized starch 1500), 525.8 ± 20.1 mg/g. Similarly, the MHCl content in the uncoated PR granules (PR-U) was as follows: F1 PR-U, 523.2 ± 0.9 mg/g; F2 PR-U, 502.3 ± 4.0 mg/g; and F3 PR-U, 510.4 ± 3.7 mg/g, demonstrating consistent drug incorporation across binder types. Statistical analysis (Welch's ANOVA and Games–Howell post hoc test) confirmed that no significant differences were observed among the F1–F3 IR and PR-U granules ($p > 0.05$). The coated PR granules exhibited MHCl contents of 362.3 ± 2.8 mg/g for F1 PR, 334.8 ± 3.6 mg/g for F2 PR, and 379.1 ± 1.7 mg/g for F3 PR. In contrast, the PR formulations showed statistically significant differences ($p < 0.05$), both relative to the IR and PR-U granules and among themselves, primarily due to the effect of the coating polymer and slight variations in granule density, binder distribution, or matrix properties, rather than the manufacturing process.

3.7.7. *Drug release*

The dissolution profiles of the IR and PR-U granules (Fig. 7a) showed clear differences driven by the presence of a disintegrant. All IR formulations released > 90 % of the MHCl within 5 min, confirming immediate-release performance due to the action of the super-disintegrant. In contrast, the PR-U granules, which lacked a disintegrant, released 44–50 % of the drug at 5 min, with release increasing gradually to 60–66 % at 45 min; this indicated that dissolution was controlled by binder hydration and gradual erosion.

The coated PR granules (F1–F3 PR, 750 mg) exhibited prolonged-release behavior (Fig. 7b) and were benchmarked against USP XR metformin tablet criteria.[50] Although defined for finished tablets, these USP criteria were used as reference standards to evaluate whether the developed granules mimicked the release of marketed XR products. The USP monograph provides multiple alternative test scenarios, reflecting formulation diversity rather than cumulative compliance. Of the 20 tests, 11 specify 500-mg tablets, one test (Test 11) specifies a 750-mg tablet, and the remaining tests do not define tablet strength. F1 PR released too quickly at intermediate time points, while F3 PR showed a burst release (> 55 % at 1 h), failing all tests. F2 PR most closely matched the USP XR profiles, fully complying with several tests (Tests 4, 12, 13, 16, and 17) and only marginally exceeding upper limits (≤ 1.9 %) at isolated intermediate points (Tests 1, 2, 3, 5, 7, 8, 9, and 20). Terminal

dissolution targets (not less than (NLT) 80–85% at 10–24 h) were consistently met, with low variability (SD 1.43–2.78; RSD < 6 %). Overall, F2 PR provided the most reproducible, extended-release profile, whereas F1 PR and F3 PR failed to control the release. Since dissolution was performed on 750-mg granules rather than tablets, the USP tests were used as qualitative benchmarks. Under this framework, F2 PR was determined to be a suitable extended-release granule system at 750 mg.

All IR formulations released > 90 % of MHCl within 5 min, demonstrating that rapid disintegration dominated the release, which left little opportunity for binder-related microstructural differences to influence dissolution.[35] In contrast, the coated PR granules were constrained by the insoluble yet permeable Eudragit® RS/RL film, making release dependent on water ingress, core hydration, and diffusion across the coating.[51] Binder type directly modulates core swelling and effective coat permeability.

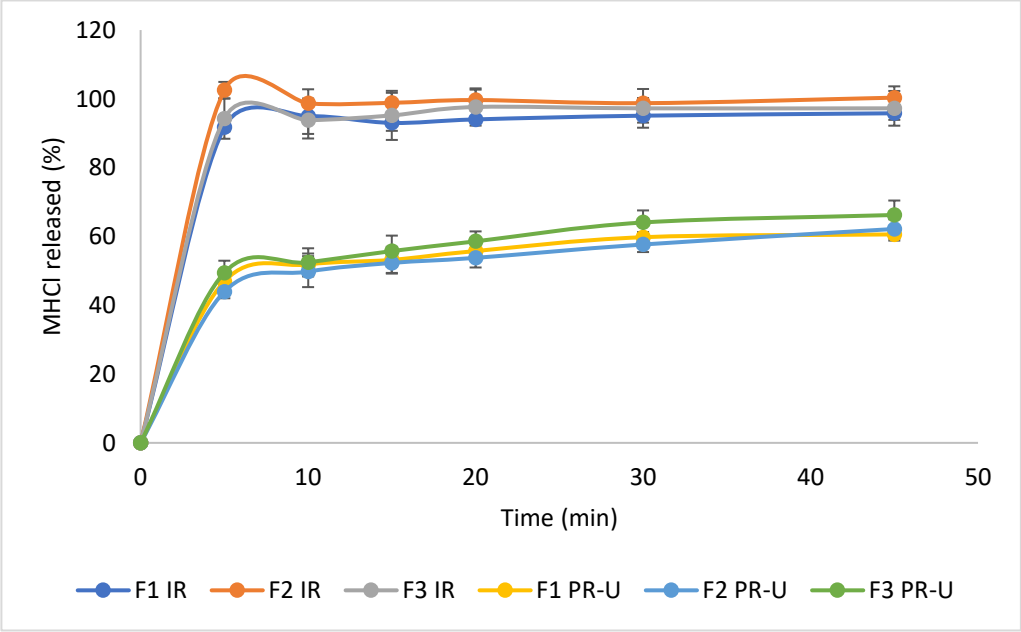

(a)

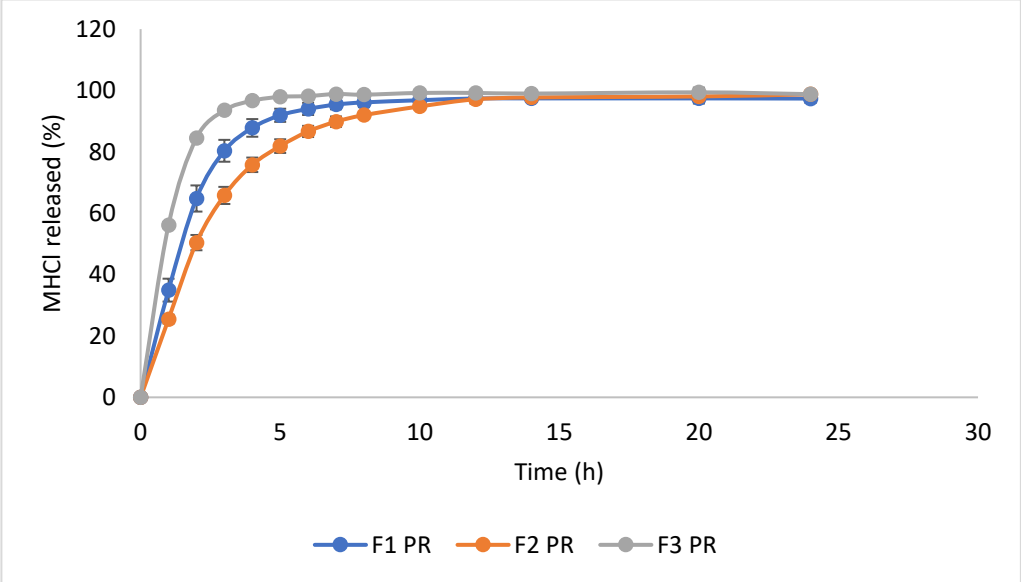

(b)

Fig. 7. Dissolution profiles of metformin hydrochloride: (a) IR and PR-U granules, and (b) PR granules. Data are presented as means ± SD (n = 3). In cases where the SD bars are not visible, the data markers exceed the size of the error bars.

The gelatin-based F2 PR granules uniquely met all acceptance windows, as gelatin forms a viscous gel network that delays aqueous channel formation, sustaining resistance during the early and intermediate phases while allowing for near-complete release during the late phase.[44] The PVP-based F1 PR formulation controlled early release but exceeded intermediate limits due to progressive PVP dissolution, which increased internal porosity and diffusion.[42] The pregelatinized starch 1500-based F3 PR granules showed the fastest burst release; rapid hydration, swelling, and wicking increased capillary penetration and potentially stressed the coating, creating microdefects.[45,48]

Overall, the binder type was identified as a critical material attribute (CMA) for the PR granules, as it governs microstructure, moisture behavior, and core–coat interactions. The main quality risk was determined to be excessive early or intermediate release rather than incomplete late release; this highlights the need for QbD-based optimization targeting hydration kinetics and porosity evolution, rather than focusing solely on the final dissolution extent.

4. CONCLUSION

Binder type strongly influenced the physicochemical properties and release behavior of high-dose metformin hydrochloride (MHCl) granules. All IR formulations achieved rapid release via disintegration; however, pronounced binder-dependent differences appeared in the PR systems constrained by a permeable polymer coating. Gelatin provided balanced performance, forming cohesive granules with controlled hydration and increased diffusion tortuosity, which sustained early and intermediate resistance while allowing complete late-stage release. In contrast, PVP and pregelatinized starch 1500 promoted faster pore formation and water uptake, thereby reducing early-release control.

These findings confirm that binder selection is a high-impact critical material attribute (CMA) for PR granules. Integrating binder-specific hydration and microstructural effects into Quality by Design (QbD) risk assessment and design space is essential for achieving robust, reproducible prolonged-release performance in high-dose, highly soluble systems.

Funding declaration: This research did not receive any specific grant from funding agencies in the public, commercial, or not-for-profit sectors.

Competing interests: The authors have no conflicts of interest to disclose.

REFERENCES

(1) Goyal, R.; Singhal, M.; Jialal, I. Type 2 Diabetes, 2023. https://www.ncbi.nlm.nih.gov/books/NBK513253/ (accessed 2026-01-27)

(2) NCD-RisC. Urgent Action Needed as Global Diabetes Cases Increase Four-Fold over Past Decades, 2024. https://www.who.int/news/item/13-11-2024-urgent-action-needed-as-global-diabetes-cases-increase-four-fold-over-past-decades (accessed 2026-01-27).

(3) Rena, G.; Hardie, D. G.; Pearson, E. R. The Mechanisms of Action of Metformin. *Diabetologia* **2017**, *60* (9), 1577–1585. https://doi.org/10.1007/s00125-017-4342-z

(4) Kanto, K.; Ito, H.; Noso, S.; Babaya, N.; Hiromine, Y.; Taketomo, Y.; Toma, J.; Niwano, F.; Yasutake, S.; Kawabata, Y.; Ikegami, H. Effects of Dosage and Dosing Frequency on the Efficacy and Safety of High-dose Metformin in Japanese Patients with Type 2 Diabetes Mellitus. *J of Diabetes Invest* **2018**, *9* (3), 587–593. https://doi.org/10.1111/jdi.12755

(5) CDER. Size, Shape, and Other Physical Attributes of Generic Tablets and Capsules: Guidance for Industry, 2022. https://www.fda.gov/media/87344/download (accessed 2026-01-27)

(6) Hummler, H.; Page, S.; Stillhart, C.; Meilicke, L.; Grimm, M.; Mannaa, M.; Gollasch, M.; Weitschies, W. Influence of Solid Oral Dosage Form Characteristics on Swallowability, Visual Perception, and Handling in Older Adults. *Pharmaceutics* **2023**, *15* (4), 1315. https://doi.org/10.3390/pharmaceutics15041315

(7) Gvozdeva, Y.; Staynova, R. Choosing the "Ideal" Oral Dosage Form for Pediatric Patients: Parents' Perspectives on Children's Preferences with a Focus on Orodispersible Tablets. *Children* **2025**, *12* (9), 1187. https://doi.org/10.3390/children12091187

(8) Mady, O. Y.; Al-Shoubki, A. A.; Donia, A. A.; Qasim, W. Metformin Hydrochloride Entrapment in Sorbitan Monostearate for Intestinal Permeability Enhancement and Pharmacodynamics. *Sci Rep* **2021**, *11* (1), 20153. https://doi.org/10.1038/s41598-021-99649-3

(9) ICH Q8(R2), 2017. https://www.ema.europa.eu/en/ich-q8-r2-pharmaceutical-development-scientific-guideline (accessed 2026-01-27).

(10) Yang, S.; Hu, X.; Zhu, J.; Zheng, B.; Bi, W.; Wang, X.; Wu, J.; Mi, Z.; Wu, Y. Aspects and Implementation of Pharmaceutical Quality by Design from Conceptual Frameworks to Industrial Applications. *Pharmaceutics* **2025**, *17* (5), 623. https://doi.org/10.3390/pharmaceutics17050623

(11) ICH Q9, 2015. https://www.ema.europa.eu/en/ich-q9-quality-risk-management-scientific-guideline (accessed 2026-01-27)

(12) USP 46 – NF 41. General Chapter〈858〉 Raman Spectroscopy. United States Pharmacopeia and National Formulary. Rockville, MD: United States Pharmacopeial Convention, 2023.

(13) Balpande, H. M.; Neha, S. R.; Milind, J. U.; Nandkishor, R. K. Compatibility Study of Metformin with Pharmaceutical Excipients. *International Journal of ChemTech Research* **2013**, *5* (4), 1684–1693.

(14) Ph. Eur. 11.0. 2.9.31 Particle Size Analysis by Laser Light Diffraction. European Pharmacopeia. EDQM, Strasbourg, 2023.

(15) USP 46 – NF 41. General Chapter 〈429〉 Light Diffraction Measurement of Particle Size. United States Pharmacopeia and National Formulary. Rockville, MD: United States Pharmacopeial Convention, 2023.

(16) Schneider, C. A.; Rasband, W. S.; Eliceiri, K. W. NIH Image to ImageJ: 25 Years of Image Analysis. *Nat Methods* **2012**, *9* (7), 671–675. https://doi.org/10.1038/nmeth.2089.

(17) McCormick, N.; Gee, M. The Measurement of the Shape of Abrasive Particles with Confocal Optical Microscopy, 2010.

(18) USP 46 – NF 41. General Chapter 〈788〉 Optical Microscopy for Particle Characterization. United States Pharmacopeia. Rockville, MD: United States Pharmacopeial Convention, 2023.

(19) ISO 4287. Profile Parameters from ISO 4287. https://guide.digitalsurf.com/en/guide-iso-4287-parameters.html. (accessed 2026-01-27)

(20) Ph. Eur. 11.0. 2.2.32 Loss on Drying. European Pharmacopeia. EDQM, Strasbourg, 2023.

(21) USP 46 – NF 41. General Chapter 〈921〉 Loss on Drying. United States Pharmacopeia and National Formulary. Rockville, MD: United States Pharmacopeial Convention, 2023.

(22) Ph. Eur. 11.0. 2.9.36 Powder Flow. European Pharmacopeia. EDQM, Strasbourg, 2023.

(23) Ph. Eur. 11.0. 2.9.34 Bulk Density and Tapped Density of Powders. European Pharmacopeia. EDQM, Strasbourg, 2023.

(24) USP 46 – NF 41. General Chapter 〈1174〉 Powder Flow. United States Pharmacopeia and National Formulary. Rockville, MD: United States Pharmacopeial Convention, 2023.

(25) USP 46 – NF 41. General Chapter 〈616〉 Bulk Density and Tapped Density of Powders. United States Pharmacopeia and National Formulary. Rockville, MD: United States Pharmacopeial Convention, 2023.

(26) Ph. Eur. 11.0. 4.1.3 Buffer Solutions, 2023.

(27) Guthrie, W. F. NIST/SEMATECH e-Handbook of Statistical Methods (NIST Handbook 151), 2020. https://doi.org/10.18434/M32189

(28) Aodah, A. H.; Fayed, M. H. H.; Alalaiwe, A.; Alsulays, B. B.; Aldawsari, M. F.; Khafagy, E.-S. Design, Optimization, and Correlation of In Vitro/In Vivo Disintegration of Novel Fast Orally Disintegrating Tablet of High Dose Metformin Hydrochloride Using Moisture Activated Dry Granulation Process and Quality by Design Approach. *Pharmaceutics* **2020**, *12* (7), 598. https://doi.org/10.3390/pharmaceutics12070598

(29) Ph. Eur. 11.0. 5.1.4. Microbiological Quality of Non-Sterile Pharmaceutical Preparations, 2023.

(30) Metry, M.; Shu, Y.; Abrahamsson, B.; Cristofoletti, R.; Dressman, J. B.; Groot, D. W.; Parr, A.; Langguth, P.; Shah, V. P.; Tajiri, T.; Mehta, M. U.; Polli, J. E. Biowaiver Monographs for Immediate Release Solid Oral Dosage Forms: Metformin Hydrochloride. *Journal of Pharmaceutical Sciences* **2021**, *110* (4), 1513–1526. https://doi.org/10.1016/j.xphs.2021.01.011.

(31) Srinivasan, S.; Elumalai, K.; Cherian, B. V.; Ramanujam, S. K. Formulation and Characterization of Metformin Hydrochloride Orodispersible Tablets with Super Disintegrants. *Intelligent Pharmacy* **2023**, *1* (3), 162–166. https://doi.org/10.1016/j.ipha.2023.06.006.

(32) Zarmpi, P.; Flanagan, T.; Meehan, E.; Mann, J.; Fotaki, N. Biopharmaceutical Aspects and Implications of Excipient Variability in Drug Product Performance. *European Journal of Pharmaceutics and Biopharmaceutics* **2017**, *111*, 1–15. https://doi.org/10.1016/j.ejpb.2016.11.004.

(33) Aneela Manzoor. Review Article: Sodium Starch Glycolate as a Super Disintegrant. *JCP* **2021**, *5* (1), 33–39. https://doi.org/10.56770/jcp2021515.

(34) Sante-2017-11668, 2019. https://www.ema.europa.eu/en/documents/scientific-guideline/annex-european-commission-guideline-excipients-labelling-and-package-leaflet-medicinal-products-human-use-sante-2017-11668-revision-1_en.pdf. (accessed 2026-01-31)

(35) Zhao, N.; Augsburger, L. L. The Influence of Granulation on Super Disintegrant Performance. *Pharmaceutical Development and Technology* **2006**, *11* (1), 47–53. https://doi.org/10.1080/10837450500463828

(36) Batra, A.; Thongsukmak, A.; Desai, D.; Serajuddin, A. T. M. The Effect of Process Variables and Binder Concentration on Tabletability of Metformin Hydrochloride and Acetaminophen Granules Produced by Twin Screw Melt Granulation with Different Polymeric Binders. *AAPS PharmSciTech* **2021**, *22* (4), 154. https://doi.org/10.1208/s12249-021-02018-6

(37) BS EN IEC 60812:2018. *Tracked Changes. Failure Modes and Effects Analysis (FMEA and FMECA)*; British Standards Institution: London, 2020.

(38) Vandevivere, L.; Denduyver, P.; Portier, C.; Häusler, O.; De Beer, T.; Vervaet, C.; Vanhoorne, V. The Effect of Binder Types on the Breakage and Drying Behavior of Granules in a Semi-Continuous Fluid Bed Dryer after Twin Screw Wet Granulation. *International Journal of Pharmaceutics* **2022**, *614*, 121449. https://doi.org/10.1016/j.ijpharm.2022.121449

(39) Sheela, N. R.; Muthu, S.; Krishnan, S. S. FTIR, FT Raman and UV-Visible Spectroscopic Analysis on Metformin Hydrochloride. *Asian Journal of Chemistry* **2010**, *22* (7), 5049–5056.

(40) Makraduli, L.; Makreski, P.; Goracinova, K.; Stefov, S.; Anevska, M.; Geskovski, N. A Comparative Approach to Screen the Capability of Raman and Infrared (Mid- and Near-) Spectroscopy for Quantification of Low-Active Pharmaceutical Ingredient Content Solid Dosage Forms: The Case of Alprazolam. *Appl Spectrosc* **2020**, *74* (6), 661–673. https://doi.org/10.1177/0003702820905367.

(41) Bayramov, F. B.; Toporov, V. V.; Chakchir, O. B.; Anisimov, V. N.; Rud, V. Y.; Glinushkin, A. P.; Bairamov, B. H. Raman Spectroscopic Characterization of Anti-Diabetic Drug Metformin Hydrochloride. *J. Phys.: Conf. Ser.* **2019**, *1400* (3), 033010. https://doi.org/10.1088/1742-6596/1400/3/033010

(42) Arndt, O.-R.; Kleinebudde, P. Roll Compaction and Tableting of High Loaded Metformin Formulations Using Efficient Binders. *AAPS PharmSciTech* **2018**, *19* (5), 2068–2076. https://doi.org/10.1208/s12249-018-1012-5

(43) Yüksel, N.; Karataş, A.; Baykara, T. Comparative Evaluation of Granules Made with Different Binders by a Fluidized Bed Method. *Drug Development and Industrial Pharmacy* **2003**, *29* (4), 387–395. https://doi.org/10.1081/DDC-120018374

(44) Abhilash, G.; Baby, B.; Rao, B.; Rajan, S.; Ramesh, K.; Kumar, G. Comparative Study on the Efficiency of Various Binder Combinations for Metformin Tablets. *Res Rev J Pharm Pharm Sci* **2013**, *2* (1), 20–24.

(45) Colorcon. Starch 1500® Pregelatinized Starch: Used as a Binder in Product/Process Development., 2009.

(46) Morkhade, D. M. Comparative Impact of Different Binder Addition Methods, Binders and Diluents on Resulting Granule and Tablet Attributes via High Shear Wet Granulation. *Powder Technology* **2017**, *320*, 114–124. https://doi.org/10.1016/j.powtec.2017.07.038

(47) Takasaki, H.; Yonemochi, E.; Ito, M.; Wada, K.; Terada, K. The Importance of Binder Moisture Content in Metformin HCL High-Dose Formulations Prepared by Moist Aqueous Granulation (MAG). *Results in Pharma Sciences* **2015**, *5*, 1–7. https://doi.org/10.1016/j.rinphs.2015.09.001

(48) Takasaki, H.; Yonemochi, E.; Ito, M.; Wada, K.; Terada, K. The Importance of Binder Moisture Content in Metformin HCL High-Dose Formulations Prepared by Moist Aqueous Granulation (MAG). *Results in Pharma Sciences* **2015**, *5*, 1–7. https://doi.org/10.1016/j.rinphs.2015.09.001

(49) Olayemi, O.; Adetunji, O.; Isimi, C. Physicochemical, Structural Characterization and Pasting Properties of Pre-Gelatinized Neorautanenia Mitis Starch. *Polim. Med.* **2021**, *51* (1), 7–16. https://doi.org/10.17219/pim/138964

(50) USP Small Molecules 3 Expert Committee. Metformin Hydrochloride Extended Release Tablets Monograph, 2021.

(51) Wulff, R.; Leopold, C. S. Coatings of Eudragit® RL and L-55 Blends: Investigations on the Drug Release Mechanism. *AAPS PharmSciTech* **2016**, *17* (2), 493–503. https://doi.org/10.1208/s12249-015-0377-y